Modern Physics Letters B
Vol. 27, No. 15 (2013) 1350115 (9 pages)

DOI: 10.1142/S0217984913501157

SUPERCONDUCTING STATE OF A PERFORATED MESOSCOPIC DISK WITH A SQUARE OR TRIANGULAR TRENCH

J. BARBA-ORTEGA
Departamento de Física, Universidad Nacional de Colombia, Carrera 30♯45-03, Bogotá, Colombia
jjbarbao@unal.edu.co

J. BARÓN JAIMEZ
Grupo Plasnamat, Instituto de Investigaciones en Materiales, Universidad Autónoma de México, DF, México
jbaron26@hotmail.com

J. ALBINO AGUIAR
Departamento de Física, Universidade Federal de Pernambuco, Recife, PE, 50670-901, Brazil
albino@df.ufpe.br

Received 18 March 2013
Revised 22 April 2013
Accepted 23 April 2013
Published 21 May 2013

In this paper, we report on the influence of a square (triangular) trench on the superconducting properties of a perforated mesoscopic sample. Effects associated to the pinning force of the hole versus the pinning by the trench and interplay between the shape of the outer boundary and the shape of the inner defects on the vortex configuration are studied for a thin disk. Using the Ginzburg–Landau theory, we calculate the magnetization, vorticity, free energy, magnetic induction, supercurrent and superconducting order parameter as a function of the applied perpendicular magnetic field. We show that only in a restricted range of the magnetic field the vortex configuration obeys the geometry of the trench. Nevertheless, we clearly demonstrate that in our sample new phenomena are possible due to competing interactions of the geometry of the sample and the added geometry of the nanoengineered trench.

Keywords: Triangular, square trench; superconducting; mesoscopics.

PACS Number(s): 74.20.De, 74.25.Bt, 74.25.Uv, 74.25.Wx

1. Introduction

Interaction between vortices and pinning centers have attracted the attention of experimental and theoretical groups due to technological applications of superconducting materials, i.e. collective locking of vortices to the pinning sites causes

enhanced critical thermodynamic parameters of the sample, intermittent motion of magnetic flux carrying vortices inside the regularly spaced weak conducting regions has been observed in the magneto-transport properties of the superconducting strip,[1,2] magnetic flux interacting with arrays of pinning sites placed on vertices of hyperbolic tessellations and are found capable of trapping vortices for a broad range of applied magnetic fluxes.[3] It is now well established that samples with arrays of holes, pillars, dots, anti-dots, etc. give rise to different kinds of vortex behavior,[4–9] in this respect superconducting samples with arrays of magnetics dots on top have been studied[10–19] founding enhancing of the critical fields, critical current and critical temperature. In previous work, we studied the superconducting matter in circular geometries. We found that the vortex configurations are strongly influenced by the geometry, boundary conditions, surface roughness and defects on the sample.[20–26] Other authors had studied the effect of surface roughness, arrays of pillars and anti-pillars, magnetic dots on superconducting films and found that the size of the sample determined the vortex configurations, the critical fields[27,28] and local density of states.[29–31] In this work, by solving the time dependent Ginzburg–Landau equations, we calculate the magnetization, free energy, vorticity, supercurrent, magnetic induction and electronic superconducting density for a thin disk with a central hole, studied frequently before for enhanced critical parameters compared to the nonperforated sample, but now containing one triangular or square trench (or barrier), and that as a function of the external magnetic field.

2. Theoretical Formalism

Let us consider a thin superconducting disk with a hole and surrounding square (triangular) trench (or barrier, as will be explained later), immersed in an insulating medium in the presence of a perpendicular uniform magnetic field H_0. The general form of the system of time dependent Ginzburg–Landau equations is:[32–34]

$$\frac{\partial\psi}{\partial t} = -(i\nabla + \mathbf{A})^2\psi + \psi(|\psi|^2 - 1)\,, \tag{1}$$

$$\frac{\partial\mathbf{A}}{\partial t} = \mathrm{Re}[\bar{\psi}(-i\nabla - \mathbf{A})\psi] - \kappa^2\nabla\times\nabla\times\mathbf{A}\,. \tag{2}$$

In Eqs. (1) and (2) dimensionless units were introduced as follows: $|\psi|$ is the order parameter in units of $|\psi_\infty(T)| = |\sqrt{\alpha(T)/\beta}|$, lengths in units of the coherence length $\xi(T)$, time in units of $t_0 = \pi\hbar/8K_BT_c$, $\mathbf{A}$ in units of $H_{c2}(T)\xi(T)$, where $H_{c2}(T)$ is the second critical field, temperature in units of the critical temperature T_c, supercurrent $J = \mathrm{Re}[\bar{\psi}(-i\nabla - \mathbf{A})\psi]$ in units of $J_0 = \hbar c^2/8\pi e\xi$; Gibbs free energy G in units of $G_0 = H_{c2}^2V/8\pi$, $\lambda(T)$ is the penetration depth.[35,36] Equation (1) for the variable thickness of the sample can be rewritten as:[37]

$$\frac{\partial\psi}{\partial t} = -\frac{1}{\tau}\,(i\boldsymbol{\nabla} + \mathbf{A}_0)\cdot\tau\,(i\boldsymbol{\nabla} + \mathbf{A}_0)\,\psi + \psi - \psi^3\,,$$

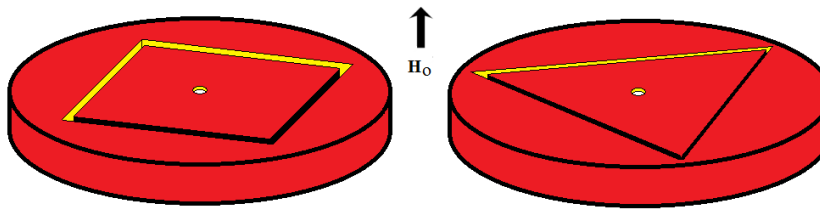

Fig. 1. Layout of the studied sample. Superconducting disk with a central hole and a square (left) or triangular (right) trench.

where $\tau(r,\theta)$ is just a function which describes the thickness of the sample. The magnetic field is considered nearly uniform inside the superconductor $\mathbf{H}_0 = \boldsymbol{\nabla} \times \mathbf{A}_0$.[21] $\tau(r,\theta) = 1$ everywhere, except at triangular and square trench position in the disk which are simulated by using $\tau = 0.9$ ($\tau > 1$ simulates a barrier of larger thickness than the rest of the sample). We simulate a mesoscopic superconducting disk of radius $R = 8\xi(T)$ with a little central hole of radius $r_i = 0.4\xi(T)$ (see Fig. 1). We will assume that the normal current density vanishes at the sample edges and at central hole, that is, $(-i\nabla - \mathbf{A})\psi \cdot \mathbf{n} = 0$, simulating superconductor/vacuum interfaces. $\mathbf{n}$ is an unit vector normal to the interfaces and directed outward the superconducting domain.

3. Results and Discussion

Figure 2 shows the (a) magnetization $-4\pi M$ (b) vorticity N, (c) Gibbs free energy G and (d) supercurrent J calculated as a function of the applied magnetic field. We simulated one internal triangular and square trench taking $\tau = 0.9$. It can be clearly noticed that this curves have a series of discontinuities signaling that one or more vortices have entered or exited the sample. It is seen from these figures that both, the first vortex penetration field and upper critical fields, are independent of the geometry of the trench in the disk, due to a large value of the τ function (close to 1 hence weak pinning force). We can appreciate vortex transition from $N \to N+4$ at $H_0 = 1.096, 1.11, 1.18, 1.23, 1.28$ for the square trench case. For the triangular trench case, there are irregular vortex transitions $N = 3 \to 5 \to 6 \to 8 \to 9 \to 11$ at low magnetic fields and a regular vortex transition starting from $N \to N+2$ (from $N = 12$ to $N = 32$) at higher fields. Also there are vortex transitions from $N \to N-1$ (from $N = 32$ to $N = 1$) in part of the downward branch of the magnetic field for both cases, excepting transitions of $10 \to 7$ at $H_0 = 0.35$ and $3 \to 1$ at $H_0 = 0.12$ for a triangular trench case and $11 \to 9 \to 7 \to 5 \to 3 \to 1$ at $H_0 = 0.33, 0.25, 0.15, 0.12$ for a square trench case. The lower and upper critical fields H_{01} and H_{03} are $H_{01} = 1.08$, $H_{03} = 1.8$ and are independent of the type of trench. With these trenches we can have a better control of the number of vortices at zero magnetic field than in a flat disk. In a previous work, a similar study was performed using a disk with a like ring circular trench, our results are consistent with this work.[24]

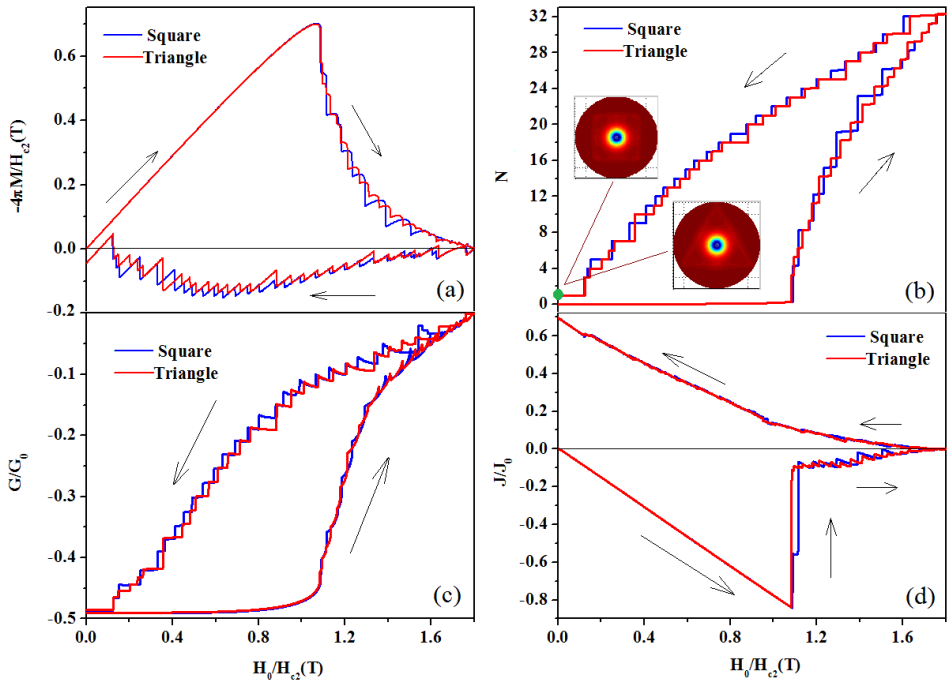

Fig. 2. (Color online) (a) Magnetization $-4\pi M$ (b) vorticity N, (c) Gibbs free energy G and (d) supercurrent J as a function of the magnetic field for the disk with a square and triangular trench.

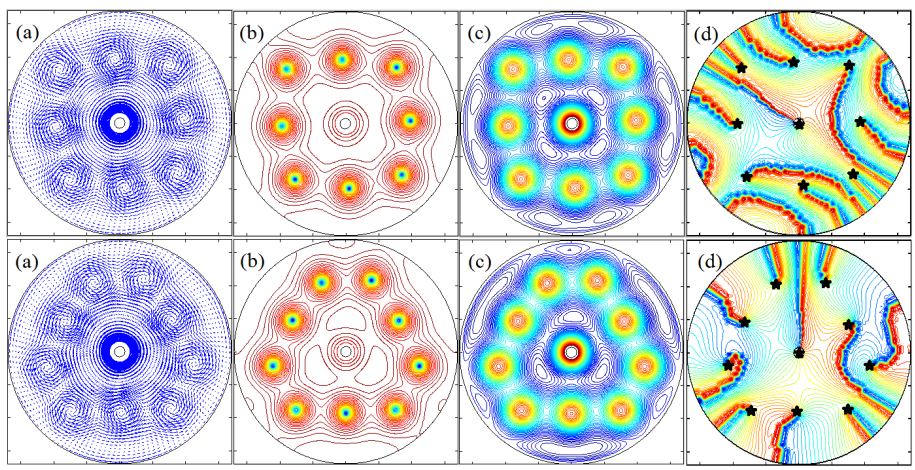

Fig. 3. (Color online) We plot (a) the supercurrent J, (b) the square modulus of the order parameter $|\psi|^2$, (c) the magnetic induction h, (d) the phase of the order parameter $\Delta\phi$ with the position of the nucleus of the vortices (black star) at $H_0 = 0.35$ in part of the downward branch of the magnetic field for a (up) square trench with $N = 9$ and triangular trench with $N = 10$. Red and blue regions represent values of the modulus of the order parameter changes from 0 to 1 respectively and 0 and 2π for the phase.

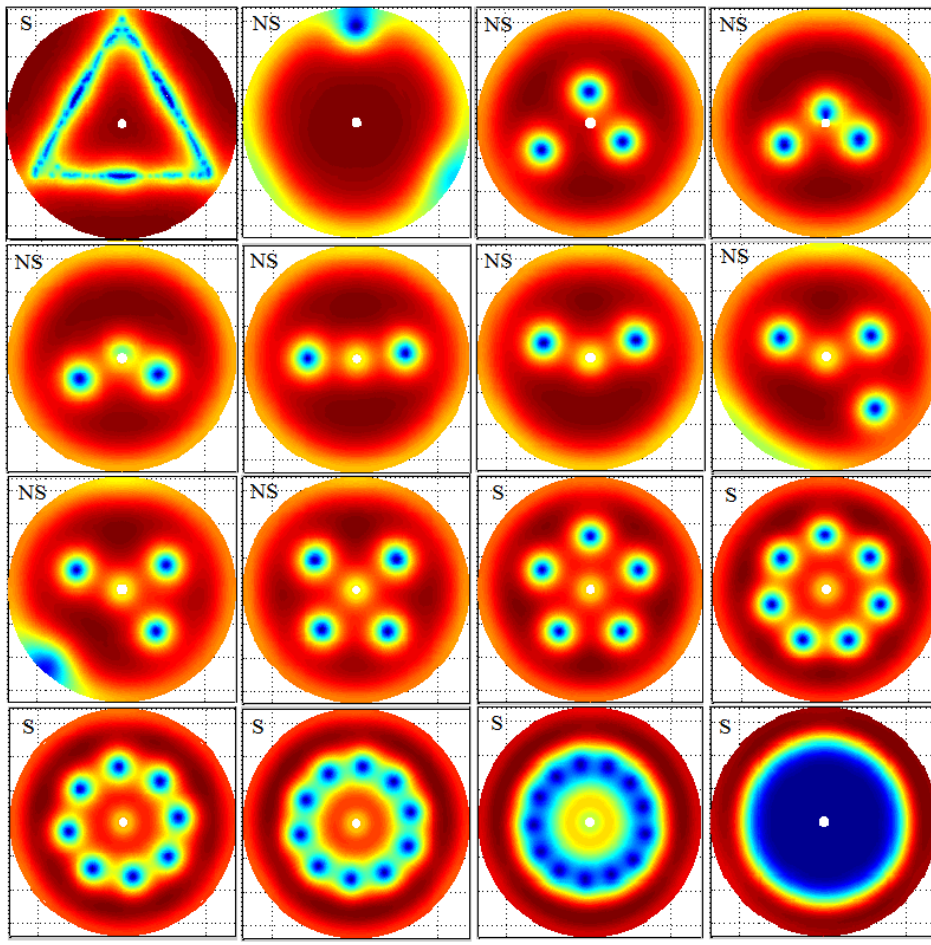

Fig. 4. Time evolution of the spatial pattern of the order parameter for a disk with a triangular trench. NS and S indicates nonstationary and stationary states, respectively.

In Fig. 3, we plot the square modulus of the order parameter, supercurrent, magnetic induction, position of the nucleus of the vortices and the order parameter phase $\Delta\phi$ for a superconducting disk at $H_0 = 0.35$ in part of the downward branch of the magnetic field, containing $N = 10$ (triangular trench) and $N = 9$ (square trench) vortices. In this magnetic field, there are vortices forming a square and triangular configuration with one single vortex at the center of the disk.

Figure 4 shows the time evolution of the spatial pattern of the order parameter for a disk with a triangular trench in a Meissner state ($H_0 = 0$). Following the panels from the left to the right and from the top to the bottom, in this order, we can see that initially three vortex nucleate the sample by every corner of the trench, increasing the magnetic field, one vortex goes to the disk center while two vortices nucleate by the south region of the disk, then they move until symmetric

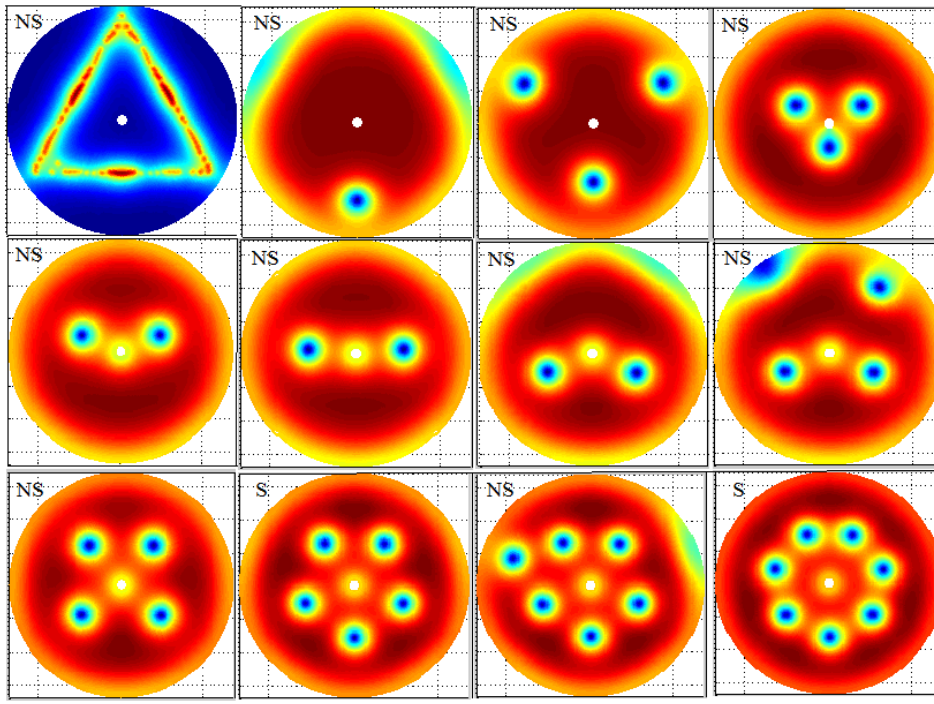

Fig. 5. Time evolution of the spatial pattern of the order parameter for a disk with a triangular barrier. NS and S indicates nonstationary and stationary states, respectively.

north region through transients states. Increasing the magnetic field, two more vortices entries at the sample forming a square configuration with $N = 4$ vortices at $H_{01} = 1.08$, the next vortices penetrate the sample at $H_{01} = 1.10$ forming a stationary state with $N = 5$. It is interesting to note that when we use $\tau = 1.1$ in our simulations (triangular barrier), the first three vortex nucleates the sample by the apices of the trench, then, one vortex goes to the disk center while two vortices remain in the sample in the north region of the disk and move until south region, as an inverse geometrical process for the vortex configurations (i.e. we observe $N = 5$ vortices forming a regular pentagon for the triangular trench case and a invert pentagon for the barrier triangle case, this process occurs both increasing and decreasing the magnetic field for all configuration at lower fields), due to anti-pinning force of the triangular barrier (Fig. 5). At higher magnetic fields, the vortex configurations for both triangular trenches are equal and occur in the same magnetic field. For the square case (Fig. 6), the four first vortices sit on the trench position forming a stable square vortex configuration with $N = 4$ at $H_{01} = 1.08$. At higher fields $H_0 > 1.14$, when more vortices come in, the geometry of the sample will prevail. As the applied field increases, all vortices collapse at the center forming a giant vortex. An additional vortex only increases the vorticity of the giant vortex (last panel of Fig. 4).

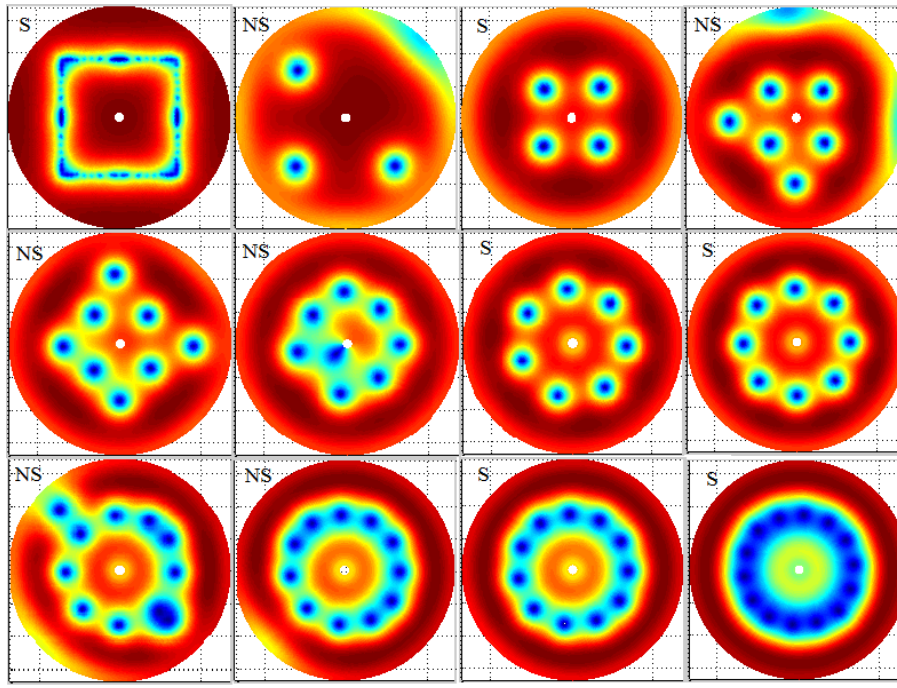

Fig. 6. Time evolution of the spatial pattern of the order parameter for a disk with a square trench. NS and S indicates nonstationary and stationary states, respectively.

4. Conclusion

We studied the effect of the geometry of a square and triangular trench on the thermodynamical properties of a mesoscopic superconducting disk with a central hole solving the time dependent Ginzburg–Landau equations. Our results have shown that the vortex state depend strongly of the geometry of the trench at low magnetic fields. We also showed that the interplay between the shape of the outer boundary and the shape of the inner trench allows a regular vortex transition from N to $N+4$ for all range of magnetic field for the square trench and $N \to N+2$ just at higher fields for a triangular trench. We observe an inverse geometrical process (π rotation in the perpendicular axis) for the vortex configuration considering a disk with a barrier triangle for equal magnetic fields. We believe that these findings are clearly relevant for the groups working or exploring the flux confinement and manipulation in nanoengineered superconductors, but also for groups studying e.g. classical, (e.g. colloidal) confined systems where similar competing interactions take place.

Acknowledgments

We would like to thank Edson Sardella and A. Barba Escobar for useful discussions.

References

1. G. R. Berdiyorov, A. R. Romaguera, M. V. Milosevic, M. Doria, L. Covaci and F. M. Peeters, *Eur. Phys. J. B* **85** (2012) 4.
2. G. R. Berdiyorov, M. V. Milosevic, M. L. Latimer, Z. L. Xiao, W. K. Kwok and F. M. Peeters, *Phys. Rev. Lett.* **109** (2012) 057004.
3. V. R. Misko and F. Nori, *Phys. Rev.* **85** (2012) 184506.
4. M. V. Milosevic, A. Kanda, S. Hatsumi, F. M. Peeters and Y. Ootuka, *Phys. Rev. Lett.* **103** (2009) 217003.
5. T. Cren, L. Serrier-Garcia, F. Debontridder and D. Roditchev, *Phys. Rev. Lett.* **107** (2011) 097202.
6. G. R. Berdiyorov, M. V. Milosevic and F. M. Peeters, *Phys. Rev. Lett.* **96** (2006) 207001.
7. G. R. Berdiyorov, M. V. Milosevic and F. M. Peeters, *Phys. Rev. B* **74** (2006) 174512.
8. G. R. Berdiyorov, V. R. Misko, M. V. Milosevic, W. Escoffier, I. V. Grigorieva and F. M. Peeters, *Phys. Rev. B* **77** (2008) 024526.
9. A. V. Silhanek, M. V. Milosevic, R. B. G. Kramer, G. R. Berdiyorov, J. Van de Vondel, R. F. Luccas, T. Puig, F. M. Peeters and V. V. Moshchalkov, *Phys. Rev. Lett.* **104** (2010) 017001.
10. D. S. Golubovic, M. V. Milosevic, F. M. Peeters and V. V. Moshchalkov, *Phys. Rev. B* **71** (2005) 180502.
11. G. Karapetrov, M. V. Milosevic, M. Iavarone, J. Fedor, A. Belkin, V. Novosad and F. M. Peeters, *Phys. Rev. B* **80** (2009) 180506.
12. A. V. Silhanek, W. Gillijns, M. V. Milosevic, A. Volodin, V. V. Moshchalkov and F. M. Peeters, *Phys. Rev. B* **76** (2007) 100502.
13. W. Gillijns, M. V. Milosevic, A. V. Silhanek, V. V. Moshchalkov and F. M. Peeters, *Phys. Rev. B* **76** (2007) 184516.
14. M. V. Milosevic and F. M. Peeters, *Phys. Rev. Lett.* **93** (2004) 267006.
15. M. V. Milosevic and F. M. Peeters, *Phys. Rev. B* **68** (2003) 024509.
16. T. Puig, E. Rosseel, L. Van Look, M. J. Van Bael, V. V. Moshchalkov, Y. Bruynseraede and R. Jonckheere, *Phys. Rev. B* **58** (1998) 5744.
17. V. Bruyndoncx, J. G. Rodrigo, T. Puig, L. Van Look, V. V. Moshchalkov and R. Jonckheere, *Phys. Rev. B* **60** (1999) 4285.
18. G. R. Berdiyorov, B. J. Baelus, M. V. Milosevic and F. M. Peeters, *Phys. Rev. B* **68** (2003) 174521.
19. M. V. Milosevic, G. R. Berdiyorov and F. M. Peeters, *Appl. Phys. Lett.* **91** (2007) 212501.
20. J. Barba-Ortega, E. Sardella, J. A. Aguiar and E. H. Brandt, *Physica C* **479** (2012) 49.
21. J. Barba-Ortega, E. Sardella and J. A. Aguiar, *Physica C* **480** (2012) 118.
22. J. Barba-Ortega, E. Sardella and J. A. Aguiar and F. M. Peeters, *Physica C* **487** (2013) 47.
23. J. Barba-Ortega, E. Sardella and J. A. Aguiar, *Supercond. Sci. Technol.* **24** (2011) 015001.
24. J. Barba-Ortega, E. Sardella and J. A. Aguiar, *Mod. Phys. Lett. B* **27**(4) (2013) 1350025.
25. J. Barba-Ortega, M. R. Joya and G. Marques, *Mod. Phys. Lett. B* **27**(11) (2013) 1350075.
26. J. Barba-Ortega, E. Sardella, J. A. Aguiar and F. M. Peeters, *Physica C* **487** (2013) 47.
27. E. Sardella and E. H. Brandt, *Supercond. Sci. Technol.* **23** (2010) 025015.

28. G. R. Berdiyorov, M. V. Milosevic and F. M. Peeters, *New J. Phys.* **11** (2009) 013025.
29. G.-Q. Zha, M. V. Milosevic, S.-P. Zhou and F. M. Peeters, *Phys. Rev. B* **84** (2011) 132501.
30. H. Sickinger, A. Lipman, M. Weides, R. G. Mints, H. Kohlstedt, D. Koelle, R. Kleiner and E. Goldobin, *Phys. Rev. Lett.* **109** (2012) 107002.
31. B. Xu, M. V. Milosevic, S.-H. Lin, F. M. Peeters and B. Janko, *Phys. Rev. Lett.* **107** (2011) 057002.
32. W. D. Gropp, H. G. Kaper, G. K. Leaf, D. M. Levine, M. Palumbo and V. M. Vinokur, *J. Comput. Phys.* **123** (1996) 254.
33. M. Tinkham, *Introduction to Superconductivity* (McGraw-Hill, New York, 1996).
34. M. V. Milosevic and R. Geurts, *Physica C* **470** (2010) 791.
35. E. Sardella, P. N. L. Filho and A. L. Malvezzi, *Phys. Rev. B* **77** (2008) 104508.
36. G. R. Berdiyorov, M. V. Milosevic, B. J. Baelus and F. M. Peeters, *Phys. Rev. B* **70** 024508 (2004) .
37. Q. Du and M. D. Gunzburger, *Physica D* **69** (1993) 215.